Highly efficient thermally activated fluorescence of a new rigid Cu(I) complex [Cu(dmp)(phanephos)]$^+$

Rafał Czerwieniec,*[a] Konrad Kowalski,*[b] and Hartmut Yersin*[a]

SUPPORTING INFORMATION

1. Instrumentation and experimental procedures

Electrospray mass spectra were recorded using a ThermoQuest Finnigan TSQ 7000 liquid-chromatography coupled mass spectrometer. ^{1}H, 13C, and COSY correlation NMR spectra were recorded on a Avance III 600 MHz spectrometer.

Photophysical measurements were performed for a diluted dichloromethane solution ($c \approx 3 \cdot 10^{-5}$ M^{-1}), a poly(methyl methacrylate) (PMMA) film containing about 1 weight% of the emitter spin-coated onto quartz glass substrates, and powder samples, respectively. The measured solutions were degassed by several pump-thaw cycles and the PMMA and solid samples were measured under inert nitrogen gas atmosphere. UV-Vis absorption spectra were registered with a Varian Cary 300 double beam spectrometer. Luminescence and excitation spectra at 300 K and at 77 K were measured with a Horiba Jobin Yvon Fluorolog 3 steady-state fluorescence spectrometer. This spectrometer was modified to allow for measurements of emission decay times. As excitation source a PicoQuant LDH-P-C-375 pulsed diode laser (λ_{exc} = 372 nm, pulse width 100 ps) was used. The emission signal was detected with a photomultiplier attached to a FAST ComTec multichannel scalar card with a time resolution of 250 ps. Decay times at other temperatures 20 K < T < 310 K were determined for powder samples deposited in a helium cryostat (Cryovac Konti Cryostat IT), in which the helium gas flow, gas pressure, and heating were controlled. The emission decay curves were recorded with a cooled photomultiplier (RCA C7164R) attached to a TR 555 tripple monochromator (Spectroscopy & Imaging GmbH) and a FAST ComTec PCI card. As excitation source, a pulsed Nd:YAG laser (IB Laser Inc., DiNY pQ 02) with an excitation wavelength of λ_{exc} = 355 nm (third harmonic) and a pulse width of about 7 ns was applied. Photoluminescence quantum yields were determined with a Hamamatsu C9920-02 system equipped with a Spectralon® integrating sphere.

Diffraction data were collected with an Oxford Diffraction Gemini Ultra CCD diffractometer with Cu-K_α radiation (λ = 1.5418 Å). The structures were resolved by direct methods (SIR-97)[1] and refined using the SHELXL-97 program.[2] The crystallographic data and refinement details are collected in Table S1.

Quantum chemical computations were performed using the Gaussian09 computer programs suite[3]. Contour plots of the resulting molecular orbitals were drawn using the GaussView program.

2. Synthesis of [Cu(dmp)(phanephos)](PF$_6$)

37 mg of [Cu(CH$_3$CN)$_4$](PF$_6$) (0.1 mmol) and 58 mg of (R_p)-(−)-4,12-bis(diphenylphosphino)-[2.2]-paracyclophane = R_p-phanephos (0.1 mmol) were dissolved in 25 ml of dry acetonitrile saturated with argon. The mixture was stirred at room temperature for 2 hours. Subsequently, 21 mg of 2,9-dimethyl-1,10-phenanthroline = dmp (0.1 mmol) were added and the mixture was stirred for another 2 hours. The solvent was evaporated and the inorganic salts were removed by passing the reaction mixture through a short column filled with neutral aluminum oxide using dichloromethane as eluent. Along with the target complex [Cu(dmp)(phanephos)](PF$_6$) a small amount of deeply red colored homoleptic complex [Cu(dmp)$_2$](PF$_6$) formed as a byproduct. Our attempts to separate these complexes by means of column chromatography turned out to be unsatisfactory. Thus, [Cu(dmp)(phanephos)](PF$_6$) was purified by several consecutive crystallizations from dichloromethane/ethyl acetate solutions (1:10 volume ratio) at -30°C. The resulting material gave correct results of elemental analyses (Found: C 64.87, H 4.67, N 2.68 %, required for $CuC_{58}H_{54}N_2O_2P_3F_6$: C 64.41, H 5.03, and N 2.59 %). The mass spectra (electro-spray) displayed a characteristic set of signals at m/z = 847.4 (M^+). The crystallizations were performed until maximal values of the emission quantum yield (ϕ_{PL} = 80 %) and decay time (τ = 14 μs) were determined for solid samples (Table 1), i.e. until emission quenching effects due to residual impurities, most of all due to the [Cu(dmp)$_2$](PF$_6$) byproduct, were minimized. Yield: 30%.

^{1}H NMR (600 MHz, CD_2Cl_2): δ = 8.62 (d, J = 8.4 Hz, 2H, dmp), 8.17 (s, 2H, dmp), 7.74 (d, J = 8.4 Hz, 2H, dmp), 7.55 (t, J = 9.0 Hz, 2H, phanephos-pCp), 7.39-7.36 (m, 4H, phanephos-Ph), 7.29 (t, J = 7.2 Hz, 2H, phanephos-Ph), 7.16 (t, J = 7.8 Hz, 4H, phanephos-Ph), 7.09 (t, J = 7.2 Hz, 2H, phanephos-Ph), 6.93 (d, J = 7.8 Hz, 2H, phanephos-pCp), 6.85 (dd, J = 8.4 Hz, 1.2 Hz, 2H, phanephos-pCp), 6.81 (t, J = 7.2 Hz, 4H, phanephos-Ph), 6.48-6.47 (m, 4H, phanephos-Ph), 3.13-3.09 (m, 2H, phanephos-pCp), 2.89-2.85 (m, 2H, phanephos-pCp), 2.76-2.72 (m, 2H, phanephos-pCp), 2.30-2.24 (m, 2H, phanephos-pCp), 1.56 (s, 6H, dmp). (pCp=paracyclophane; Ph=phenyl; Fig. S1)

^{31}P NMR (121 MHz, CD_2Cl_2): δ = -2.19(s, phanephos), -143.90 (hept, PF$_6$)

The same procedure was applied to the second enantiomer of the phanephos ligand: (S_p)-(+)-4,12-bis(diphenylphosphino)-[2.2]-paracyclophane = S_p-phanephos affording [Cu(dmp)(S_p-phanephos)](PF$_6$).

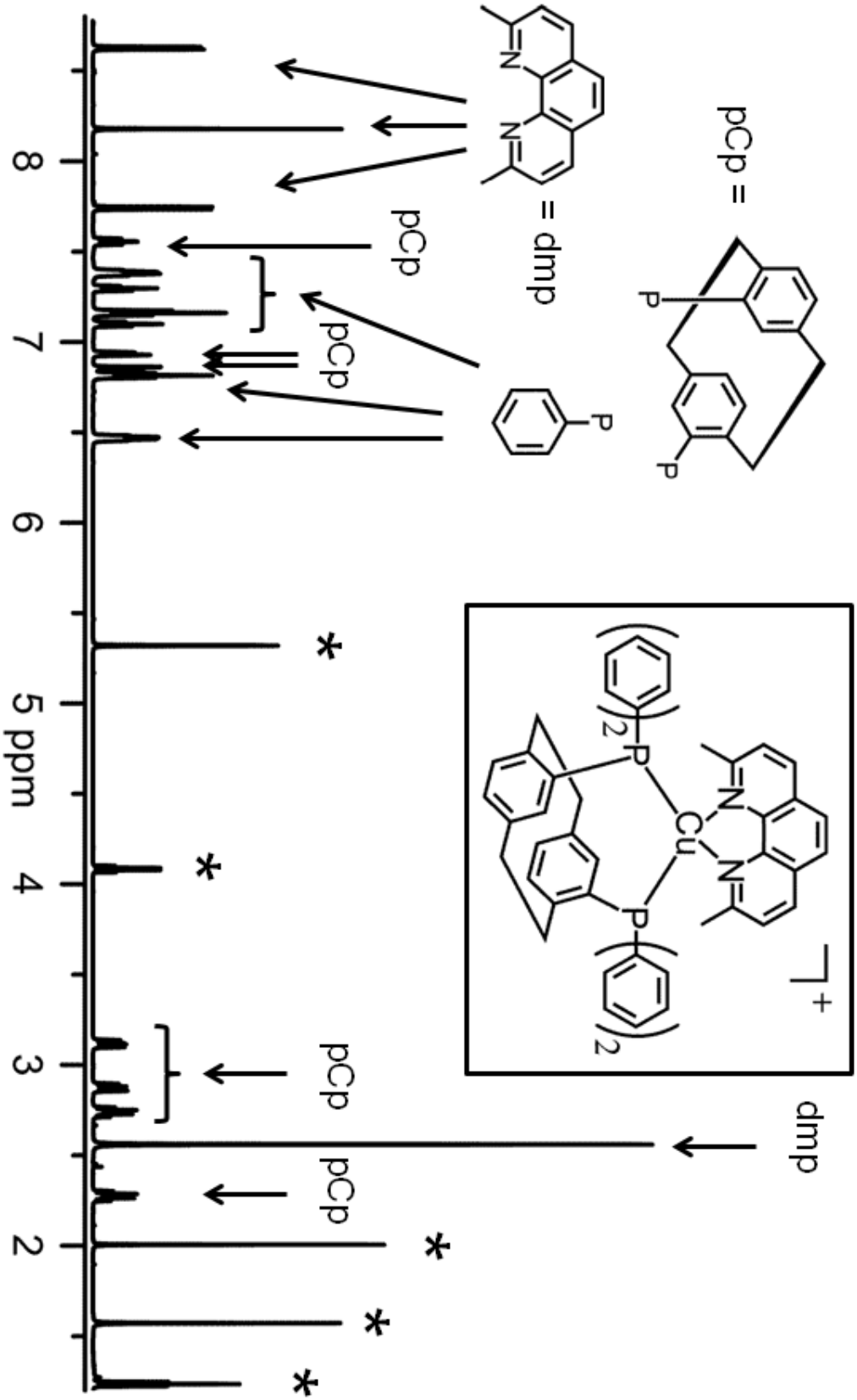

Figure S1. ^{1}H NMR spectrum for [Cu(dmp)(phanephos)](PF_6) recorded in CD_2Cl_2 (c ≈ 12 M). Signals marked with an asterisk are due to protons of $CDHCl_2$, H_2O, and ethyl acetate.

3. Crystal structures

Crystals suitable for x-ray analysis were obtained from dichloromethane/ethyl acetate (1:10 volume ratio) solutions at -30°C. [Cu(dmp)(phanephos)](PF_6) crystallizes in the non-centrosymmetric orthorhombic crystal system. In addition to the $[Cu(dmp)(phanephos)]^+$ and PF_6^- ions, the asymmetric unit contains also one ethyl acetate solvent molecule. The molecular structures of the two enantiomeric [Cu(dmp)(R_p-phanephos)]$^+$ and [Cu(dmp)(S_p-phanephos)]$^+$ ions and atom numbering schemes are displayed in Fig. S2. Relevant bond lengths and angles are summarized in Table S2.

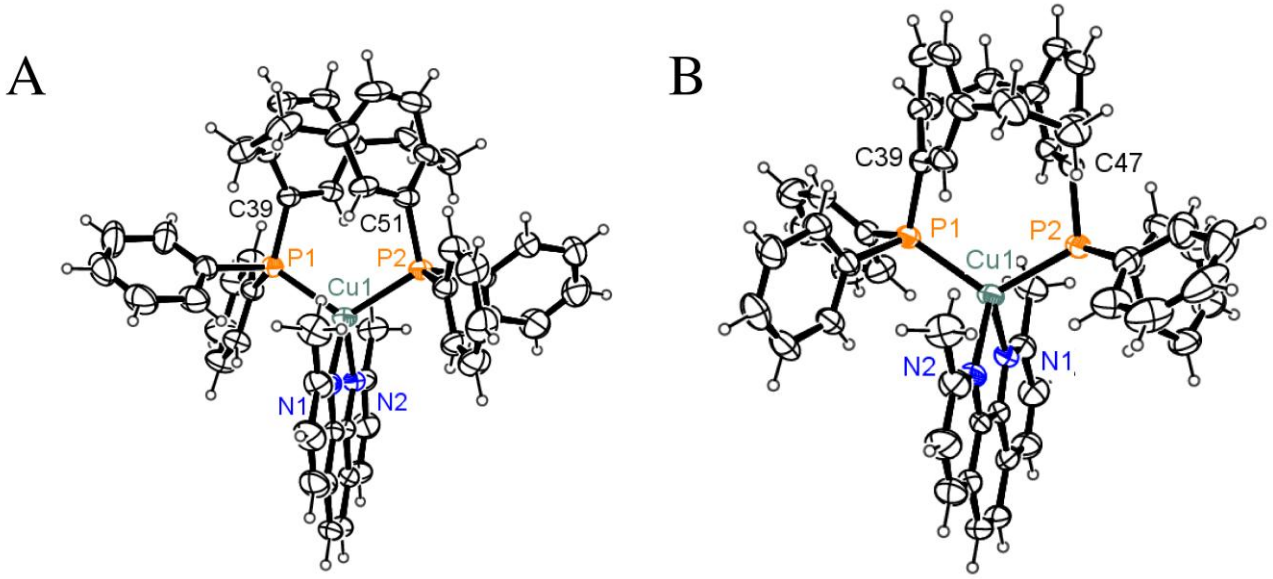

Figure S2. Molecular views (thermal ellipsoids at the 50% probability level) on the $[Cu(dmp)(phanephos)]^+$ ions: (A) phanephos enantiomer R_p (B) phanephos enantiomer S_p. The PF_6^- ions and solvent molecules are omitted for clarity.

Table S1. Crystal data, data collection, and structure refinement details.

	[Cu(dmp)(R_p-phanephos)](PF_6) × $CH_3CO_2C_2H_5$	[Cu(dmp)(S_p-phanephos)](PF_6) × $CH_3CO_2C_2H_5$
crystal shape	prism	prism
crystal color	faint yellow	faint yellow
empirical formula	C_{58} H_{54} Cu F_6 N_2 O_2 P_3	C_{58} H_{54} Cu F_6 N_2 O_2 P_3
formula weight [g mol^{-1}]	1081.49	1081.49
crystal size [mm]	0.6690/ 0.5778/ 0.3652	0.3145/ 0.1752/ 0.1534
crystal system	orthorhombic	orthorhombic
space group	P 21 21 21	P 21 21 21
a [Å]	16.4869(2)	16.5204(4)
b [Å]	17.65670(17)	17.5982(3)
c [Å]	18.69160(19)	18.7370(3)
α [°]	90	90
β [°]	90	90
γ [°]	90	90
cell volume [$Å^3$]	5441.21(10)	5447.40(18)
Z	4	4
density [g cm^{-1}]	1.320	1.319
absorption coefficient [mm^{-1}]	1.934	1.931
F(000)	2240	2240
T [K]	293	297
λ [Å]	1.54184	1.54184
Θ range [°]	3.44 − 63.39	3.4426 − 63.4135
reflections collected	19860	22288
unique reflections	8583	8045
observed reflections [$I > 2\sigma(I)$]	8263	7179
absorption correction	analytical	analytical
GOF	1.032	1.026
final R_1 [$I \geq 2\sigma(I)$]	0.0399	0.0457
wR_2	0.1089	0.1190

Table S2. Selected bond lengths [Å] and angles [°] for [Cu(dmp)(phanephos)]$^+$. Atom numbering is given in Fig. S1.

[Cu(dmp)(R_p-phanephos)]$^+$		[Cu(dmp)(S_p-phanephos)]$^+$	
Cu1-N1	2.108(3)	Cu1-N2	2.105(3)
Cu1-N2	2.115(2)	Cu1-N1	2.116(3)
Cu1-P1	2.3142(8)	Cu1-P1	2.3147(10)
Cu1-P2	2.3049(8)	Cu1-P2	2.3046(11)
P1-C39	1.836(3)	P1-C39	1.828(4)
P2-C51	1.825(3)	P2-C47	1.827(4)
P1-P2	3.912	P1-P2	3.908
N1-Cu1-N2	80.20(10)	N1-Cu1-N2	80.28(13)
P1-Cu1-P2	115.74(3)	P1-Cu1-P2	115.58(4)
P1-Cu1-N1	117.04(7)	P1-Cu1-N1	117.99(9)
P1-Cu1-N2	109.58(7)	P1-Cu1-N2	112.01(10)
P2-Cu1-N1	111.93(8)	P2-Cu1-N2	116.86(10)
P2-Cu1-N2	117.61(7)	P2-Cu1-N1	109.47(9)
P1-P2-N2-N1	71.39	P1-P2-N1-N2	71.85

[Cu(dmp)(phanephos)]$^+$ exhibits a four-coordinated metal center with a distorted tetrahedral geometry. The P-Cu-P and N-Cu-N angles of about 116° and 80°, respectively, strongly deviate from the value of 109° of an ideal tetrahedron. This reflects distinctly different steric requirements of the phanephos and dmp ligands. In particular, the P-Cu-P angle formed for the phanephos ligand matches with the largest value reported for the "wide bite-angle" pop ligand that coordinates with a P-Cu-P angle in the range between 108° and 116°.[4,] The rigid paracyclophane group and the two diphenylphosphine functions separated by a P1-P2 distance of about 3.9 Å form a firm semi-cage occupied by the metal ion and the dmp ligand. Moreover, the overall bulkiness of the phenaphos ligand and the methyl groups of dmp around the metal center seem to provide a good shielding of the potentially (photo-) reactive metal centre from direct contact with solvent molecules.

4. Electronic transitions – TD-DFT calculations.

Time-dependent density functional calculations were performed for the molecular geometry of [Cu(dmp)(R_p-phanephos)]$^+$ resulting from the x-ray diffraction measurements. Five lowest energy singlet and triplet transitions were calculated using the B3LYP[5] functional and the SVP[6] atomic orbital basis set for all atoms. The results are summarized in Table S3 and Figure S3. In particular, the lowest excited states S_1 and T_1 are predicted to have a distinct charge-transfer character, where electron density is shifted from the metal center and the aromatic system of the phanephos ligand to the dmp ligand. This result substantiates the MLCT nature of the S_1 and T_1 states. The calculated energy separation between the two states $\Delta E(S_1-T_1)$ amounts to 1540 cm^{-1}. However, the TD-DFT computation has been carried out for the ground state conformation, regardless of any geometry reorganization taking place upon excitation. Thus, taken this approximation and also in view of the known problems regarding the prediction of transition energies of charge-transfer excited states by TD-DFT,[7] the calculated singlet-triplet splitting, being about 50% larger than the $\Delta E(S_1-T_1)$ value determined experimentally (from the decay time analysis), is regarded to be in a fair agreement.

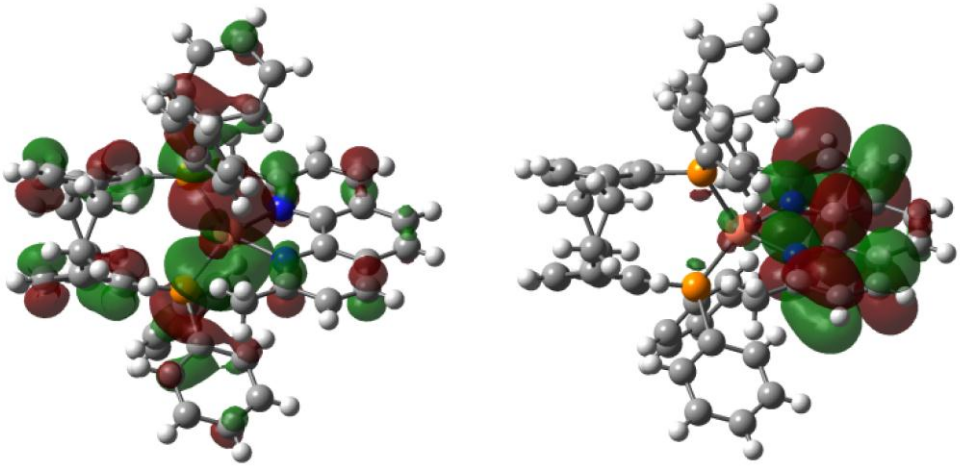

Figure S3. Contour plots of the natural transition orbitals[8] obtained for the lowest excited singlet state S_1 of [Cu(dmp)(phanephos)]$^+$ on the B3LYP/SVP TD-DFT theory level.

Table S3. Calculated energy levels, oscillator strengths (*f*), and orbital analyses for the five lowest singlet and triplet transitions in $[Cu(dmp)(phanephos)]^+$.

transition	energy [cm^{-1}]	*f*	assignement	character
$S_0 \rightarrow T_1$	21130	0	HOMO → LUMO (92 %)	d-π^*_{dmp}
$S_0 \rightarrow S_1$	22670	0.0621	HOMO → LUMO (78 %)	d-π^*_{dmp}
$S_0 \rightarrow T_2$	23550	0	HOMO − 3→ LUMO + 1 (70 %) HOMO → LUMO + 1 (14 %)	d-π^*_{dmp}
$S_0 \rightarrow T_3$	23570	0	HOMO → LUMO + 1 (46 %) HOMO − 3→ LUMO (22 %)	d-π^*_{dmp}
$S_0 \rightarrow T_4$	24300	0	HOMO – 1 → LUMO + 6 (22 %) HOMO → LUMO + 2 (18 %) HOMO – 4 → LUMO + 2 (14 %) HOMO – 1 → LUMO + 4 (9 %) HOMO – 5 → LUMO + 11 (6 %)	d/π_{phan}-π^*_{phan}
$S_0 \rightarrow T_5$	24390	0	HOMO – 2 → LUMO (50 %) HOMO – 1 → LUMO (42 %)	d/π_{phan}-π^*_{dmp}
$S_0 \rightarrow S_2$	24750	0.0024	HOMO – 3 → LUMO (87 %) HOMO – 1 → LUMO (5 %)	d/π_{phan}-π^*_{dmp}
$S_0 \rightarrow S_3$	25040	0.0036	HOMO – 1→ LUMO (48 %) HOMO – 2 → LUMO (42 %) HOMO – 3 → LUMO (6 %)	d/π_{phan}-π^*_{dmp}
$S_0 \rightarrow S_4$	25240	0.0088	HOMO → LUMO + 2 (95 %)	d-π^*_{dmp}
$S_0 \rightarrow S_5$	25490	0.0004	HOMO – 2→ LUMO (52 %) HOMO – 1 → LUMO (46 %)	d/π_{phan}-π^*_{dmp}

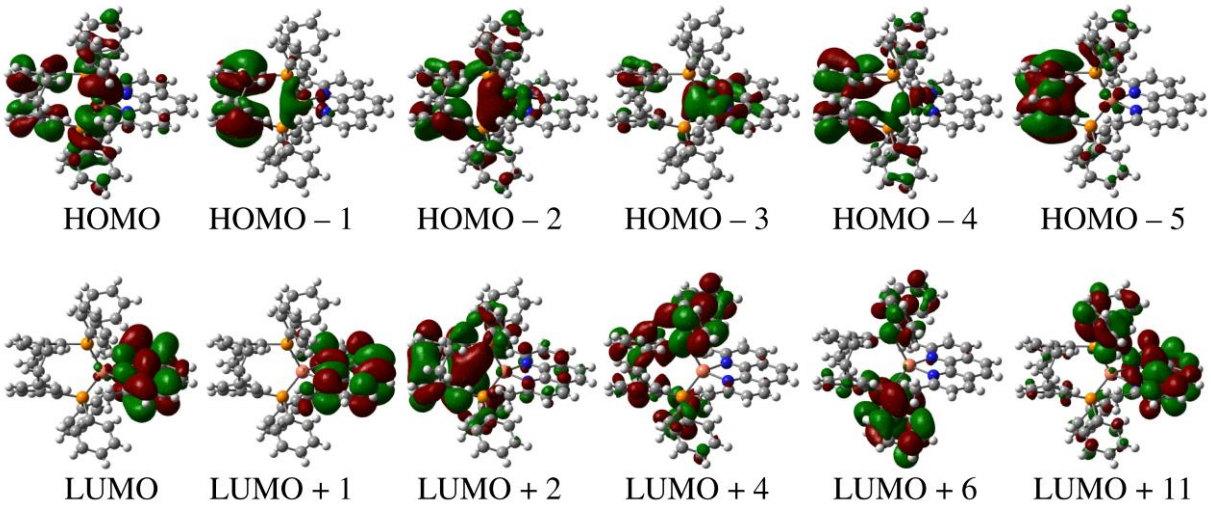

Figure S4. Molecular orbitals (active space) important for the low-energy electronic transitions of $[Cu(dmp)(phanephos)]^+$ listed in Table S3.

5. Estimation of the radiative decay rate of the $S_1 \rightarrow S_0$ transition.

For a two-state model, i.e. the ground state and an excited state, spontaneous emission probability is directly proportional to the corresponding absorption strength (molar extinction) and to the third power of the energy separation between these states. The relationship between the radiative decay rate of the spontaneous $S_1 \rightarrow S_0$ emission, $k_r(S_1)$, and the $S_0 \rightarrow S_1$ absorption strength can be expressed as:[9]

$$k_r(S_1) = 8 \cdot \ln 10 \cdot \pi \cdot c \cdot n^2 \cdot N_A{}^{-1} \cdot \left\langle \bar{\nu}_{fl}{}^{-3} \right\rangle_{av}^{-1} \cdot \int \frac{\varepsilon(\bar{\nu}_{abs})}{\bar{\nu}_{abs}} d\bar{\nu}_{abs} \qquad \text{(S1)}$$

where c is the speed of light in vacuum, N_A is the Avogadro constant, and n is the refractive index of the medium. $\left\langle \bar{\nu}_{fl}{}^{-3} \right\rangle_{av}^{-1}$ represents the reciprocal of the mean value of the third power of the fluorescence energy $\bar{\nu}_{fl}$ [cm^{-1}] (weighted with the emission intensity at each $\bar{\nu}_{fl}$ value of the fluorescence spectrum) and the integral $\int \frac{\varepsilon(\bar{\nu}_{abs})}{\bar{\nu}_{abs}} d\bar{\nu}_{abs}$ represents the absorption strength of the $S_0 \rightarrow S_1$ absorption band. $\varepsilon(\bar{\nu}_{abs})$ is the molar absorption coefficient at a given energy $\bar{\nu}_{abs}$. If $\left\langle \bar{\nu}_{fl}{}^{-3} \right\rangle_{av}^{-1}$ is approxiamted by the third power of the emission maximum $\bar{\nu}_{max}{}^3$, eq. (S1) can be expressed as:

$$k^r(S_1) = const \cdot n^2 \cdot \bar{\nu}_{max}{}^3 \cdot \int \frac{\varepsilon(\bar{\nu}_{abs})}{\bar{\nu}_{abs}} d\bar{\nu}_{abs} \qquad (S2)$$

with $const = 2.88 \cdot 10^{-12}$ s^{-1} mol cm.

From an integration of the lowest absorption band of [Cu(dmp)(phanephos)](PF_6) dissolved in dichloromethane (n = 1.42) measured at ambient temperature an approximate value of $\int \frac{\varepsilon(\bar{\nu}_{abs})}{\bar{\nu}_{abs}} d\bar{\nu}_{abs} = 3.7 \cdot 10^5$ cm^2 mol^{-1} is be obtained (Fig. S5). For $\bar{\nu}_{max}$, a value of 17500 cm^{-1} (CH_2Cl_2, 300 K) is taken. Thus, a radiative decay rate of the spontaneous $S_1 \rightarrow S_0$ fluorescence of $k_r(S_1) \approx 1.2 \cdot 10^7$ s^{-1}, corresponding to a radiative decay time for the $S_1 \rightarrow S_0$ transition of $\tau^r \approx 80$ ns, is obtained.

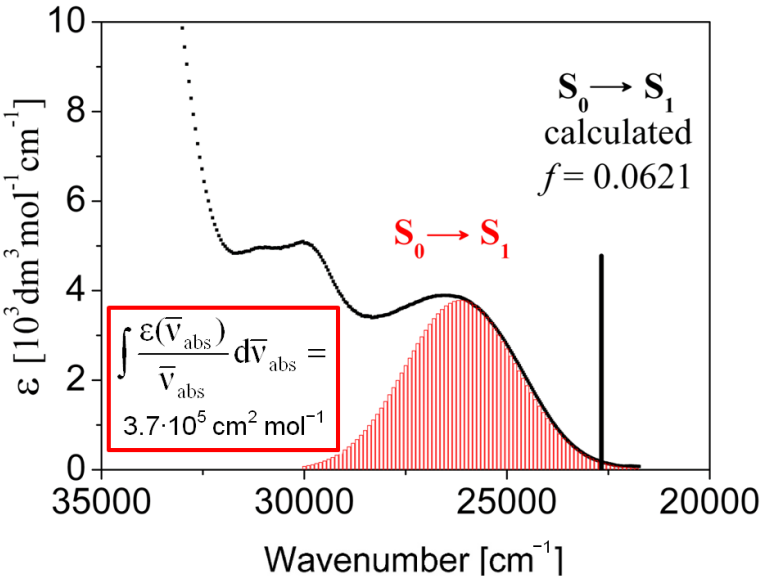

Figure S5. Ambient-temperature absorption spectrum of [Cu(dmp)(phanephos)](PF_6) in CH_2Cl_2. (Compare Fig 1.) The red-shaded area marks approximately the $S_0 \rightarrow S_1$ absorption band. The calculated 0-0 lines energy (TD-DFT level) of the $S_0 \rightarrow S_1$ transition is also displayed. The TD-DFT calculations reveal a series of additional charge-transfer transitions at energies close to that of the $S_0 \rightarrow S_1$ transition. However, according to their very small oscillator strengths *f* (Table S3), they were neglected for the approximate analysis of the lowest-energy ^{1}MLCT absorption strength.

References:

S1 A. Altomare, G. Cascarano, C. Giacovazzo, A. Guagliardi, *J. Appl. Crystallogr.*, 1993, **26**, 343.

S2 G. M. Sheldrick, SHELXL-97. *Program for crystal structure refinement*, University of Göttingen, Germany, 1997.

S3 Gaussian09W, Version 8.0, M. J. Frisch, G. W. Trucks, H. B. Schlegel, G. E. Scuseria, M. A. Robb, J. R. Cheeseman, G. Scalmani, V. Barone, B. Mennucci, G. A. Petersson, H. Nakatsuji, M. Caricato, X. Li, H. P. Hratchian, A. F. Izmaylov, J. Bloino, G. Zheng, J. L. Sonnenberg, M. Hada, M. Ehara, K. Toyota, R. Fukuda, J. Hasegawa, M. Ishida, T. Nakajima, Y. Honda, O. Kitao, H. Nakai, T. Vreven, J. A. Montgomery, Jr., J. E. Peralta, F. Ogliaro, M. Bearpark, J. J. Heyd, E. Brothers, K. N. Kudin, V. N. Staroverov, R. Kobayashi, J. Normand, K. Raghavachari, A. Rendell, J. C. Burant, S. S. Iyengar, J. Tomasi, M. Cossi, N. Rega, J. M. Millam, M. Klene, J. E. Knox, J. B. Cross, V. Bakken, C. Adamo, J. Jaramillo, R. Gomperts, R. E. Stratmann, O. Yazyev, A. J. Austin, R. Cammi, C. Pomelli, J. W. Ochterski, R. L. Martin, K. Morokuma, V. G. Zakrzewski, G. A. Voth, P. Salvador, J. J. Dannenberg, S. Dapprich, A. D. Daniels, Ö. Farkas, J. B. Foresman, J. V. Ortiz, J. Cioslowski, and D. J. Fox, Gaussian, Inc., Wallingford CT, 2009.

S4 (a) M. G. Crestani, G. F. Manbeck, W. W. Brennessel, T. M. McCormick, R. Eisenberg, *Inorg. Chem*., 2011, **50**, 7172. (b) R. Venkateswaran, M. S. Balakrishna, S. M. Mobin, H. M. Tuononen, *Inorg. Chem*., 2007, **46**, 6535. (c) D. G. Cuttel, S.-M. Kuang, P. E. Fanwick, D. R. McMillin, R. A. Walton, *J. Am. Chem. Soc*., 2001, **124**, 6. (d) S.-M. Kuang, D. G. Cuttel, D. R. McMillin, P. E. Fanwick, R. A. Walton, *Inorg. Chem*., 2002, **41**, 3313. (e) J. Xu, D. Yun, B. Lin, *Synth.Met*., 2011, **161**, 1276. (f) P. Aslanidis, P. J. Cox, A. C. Tsipis, *Dalton Trans*., 2010, **39**, 10238. (g) C. W. Hsu, C.-C. Lin, M.-W. Chung, Y. Chi, G.-H. Lee, P.-T. Chou, C.-H. Chang, P.-Y. Chen, *J. Am. Chem. Soc*., 2011, **133**, 12085. (h) R. Czerwieniec, J. Yu, H. Yersin, *Inorg. Chem*., 2011, **50**, 8293. (i) L. Qin, Q. Zhang, W. Sun, J. Wang, C. Lu, Y. Cheng, L. Wang, *Dalton Trans*. 2009, 9388. (j) Q. Zhang, J. Ding, Y. Cheng, L. Wang, Z. Xie, X. Jing, F. Wang, *Adv. Funct. Mater*., 2007, **17**, 2983. (k) C. Femoni, S. Muzzioli, A. Palazzi, S. Stagni, S. Zacchini, F. Monti, G. Accorsi, M. Bolognesi, N. Armaroli, M. Massi, G. Valenti, M. Marcaccio, *Dalton Trans*., 2013, **42**, 997.

S5 (a) A. D. Becke, *J. Chem. Phys*., 1993, **98**, 5648. (b) P. J. Stephens, F. J. Devlin, C. F. Chabalowski, M. J. Frisch, *J. Phys. Chem*., 1994, **98**, 11623.

S6 A. Schaefer, H. Horn, R. Ahlrichs, *J. Chem. Phys.*, 1992, **97,** 2571.

S7 (a) A. Dreuw, M. Head-Gordon, *J. Am. Chem. Soc*., 2004, **126**, 4007. (b) P. Wiggins, J. A. G. Williams, D. J. Tozer, *J. Chem. Phys*., 2009, **131**, 091101. (c) Z.-L. Cai, M. J. Crossley, J. R. Reimers, R. Kobayashi, R. D. Amos, *J. Phys. Chem. B*, 2006, **110**, 15624.

S8 R. L. Martin, *J. Chem. Phys.*, 2003, **118,** 4775.

S9 S. J. Strickler, R. A. Berg, *J. Chem. Phys.*, 1962, **37**, 814.